



## Wind reduction by aerosol particles

Mark Z. Jacobson<sup>1</sup> and Yoram J. Kaufman<sup>2,3</sup>

Received 10 August 2006; revised 12 October 2006; accepted 22 November 2006; published 27 December 2006.

[1] Aerosol particles are known to affect radiation, temperatures, stability, clouds, and precipitation, but their effects on spatially-distributed wind speed have not been examined to date. Here, it is found that aerosol particles, directly and through their enhancement of clouds, may reduce near-surface wind speeds below them by up to 8% locally. This reduction may explain a portion of observed “disappearing winds” in China, and it decreases the energy available for wind-turbine electricity. In California, slower winds reduce emissions of wind-driven soil dust and sea spray. Slower winds and cooler surface temperatures also reduce moisture advection and evaporation. These factors, along with the second indirect aerosol effect, may reduce California precipitation by 2–5%, contributing to a strain on water supply. **Citation:** Jacobson, M. Z., and Y. J. Kaufman (2006), Wind reduction by aerosol particles, *Geophys. Res. Lett.*, 33, L24814, doi:10.1029/2006GL027838.

### 1. Introduction

[2] In theory, aerosol particles should decrease wind speeds below them. During the day, absorbing and scattering aerosol particles increase stability by reducing solar radiation to the ground [Bergstrom and Viskanta, 1973; Venkatram and Viskanta, 1977; Ackerman, 1977; Jacobson, 1998, Figures 8a and 8b]. Soot and soildust absorb solar absorption, heating the air and enhancing stability further. During the day and night, all boundary-layer particles radiatively warm the surface, decreasing stability there, but radiatively cool the air above them, creating or enhancing an inversion 0.4–1 km above ground [e.g., Bergstrom and Viskanta, 1973, Figure 4; Ackerman et al., 1976, Figure 4; Jacobson, 1998, Figure 8c]. An increase in the air’s stability due to aerosols or any other mechanism reduces vertical turbulence, reducing the vertical flux of horizontal momentum [Riehl, 1972; Zdunkowski and McQuage, 1972; Zdunkowski et al., 1976; Arya, 1988; Archer and Jacobson, 2003]. Since winds are generally faster aloft than at the surface, reduced vertical fluxes of winds reduce transfer of fast winds aloft to the surface, slowing surface winds relative to those aloft. Conversely, enhanced afternoon instability increases the downward transport of fast winds, explaining why near-surface winds often peak in the afternoon [Riehl, 1972].

[3] Here, the effects of aerosol particles on spatially-distributed wind speeds and the resulting feedbacks to precipitation, water supply, and wind energy are examined with a 3-D computer model (to determine cause and effect) and supporting evidence from satellite data (to determine correlation).

### 2. Methods

[4] First, MODIS satellite aerosol optical depth retrievals were analyzed with National Center for Environmental Prediction (NCEP) reanalysis wind speeds over the South Coast Air Basin (SCAB) in California during February and August, 2002–2004. Averaged over the basin during August, NCEP near surface wind speeds over land decreased from 4.2 m/s, when the aerosol optical depth (AOD) was in the lowest third of those measured, to 3.5 m/s (17% decrease) when the AOD was in the highest third. For February, wind speeds decreased over land from 7.5 m/s at low AOD to 6.5 m/s (13% decrease) at high AOD. Overall, a negative correlation was found between AOD and near-surface wind speed, but this does not prove cause and effect.

[5] To determine whether aerosol particles can reduce wind speed, numerical model experiments were undertaken for the same airshed, SCAB, with the global-through-urban computer model GATOR-GCMOM [Jacobson, 1997, 2001, 2002, 2003, 2004], described in the auxiliary material<sup>1</sup>. The model treated three nested domains: global (4°-SN × 5°-WE), California (0.2° × 0.15°), and SCAB (0.045° × 0.05°). In the California and SCAB domains, the model treated the 3-D evolution and transport of size-resolved clouds and precipitation from aerosol particles inclusions (M. Z. Jacobson et al., Examining feedbacks of aerosols to urban climate with a model that treats 3-D clouds with aerosol inclusions, submitted to *Journal of Geophysical Research*, 2006, available at [www.stanford.edu/group/efmh/jacobson/iie.html](http://www.stanford.edu/group/efmh/jacobson/iie.html)) (hereinafter referred to as Jacobson et al., submitted manuscript, 2006). The first and second indirect aerosol effects were treated without cloud or aerosol parameterization.

[6] The model was first run for February and August 1999 with and without emission of anthropogenic aerosol particle and precursor gases (AAPPG) in the SCAB domain. Precursor gases removed included anthropogenic SO<sub>x</sub>, NO<sub>x</sub>, NH<sub>3</sub>, and speciated organics gases, but not CO<sub>2</sub>, CH<sub>4</sub>, N<sub>2</sub>O, or CFCs. Particle emissions removed included black and organic carbon, sulfate, and nitrate. Gridded, time-dependent emissions were derived from the 1999 U.S. National Emission Inventory (U.S. Environmental Protection Agency, 2006, <http://www.epa.gov/ttn/chief/>). Jacobson et al. (submitted manuscript, 2006) compares model values

<sup>1</sup>Department of Civil and Environmental Engineering, Stanford University, Stanford, California, USA.

<sup>2</sup>Laboratory for Atmospheres, NASA Goddard Space Flight Center, Greenbelt, Maryland, USA.

<sup>3</sup>Deceased 31 May 2006.

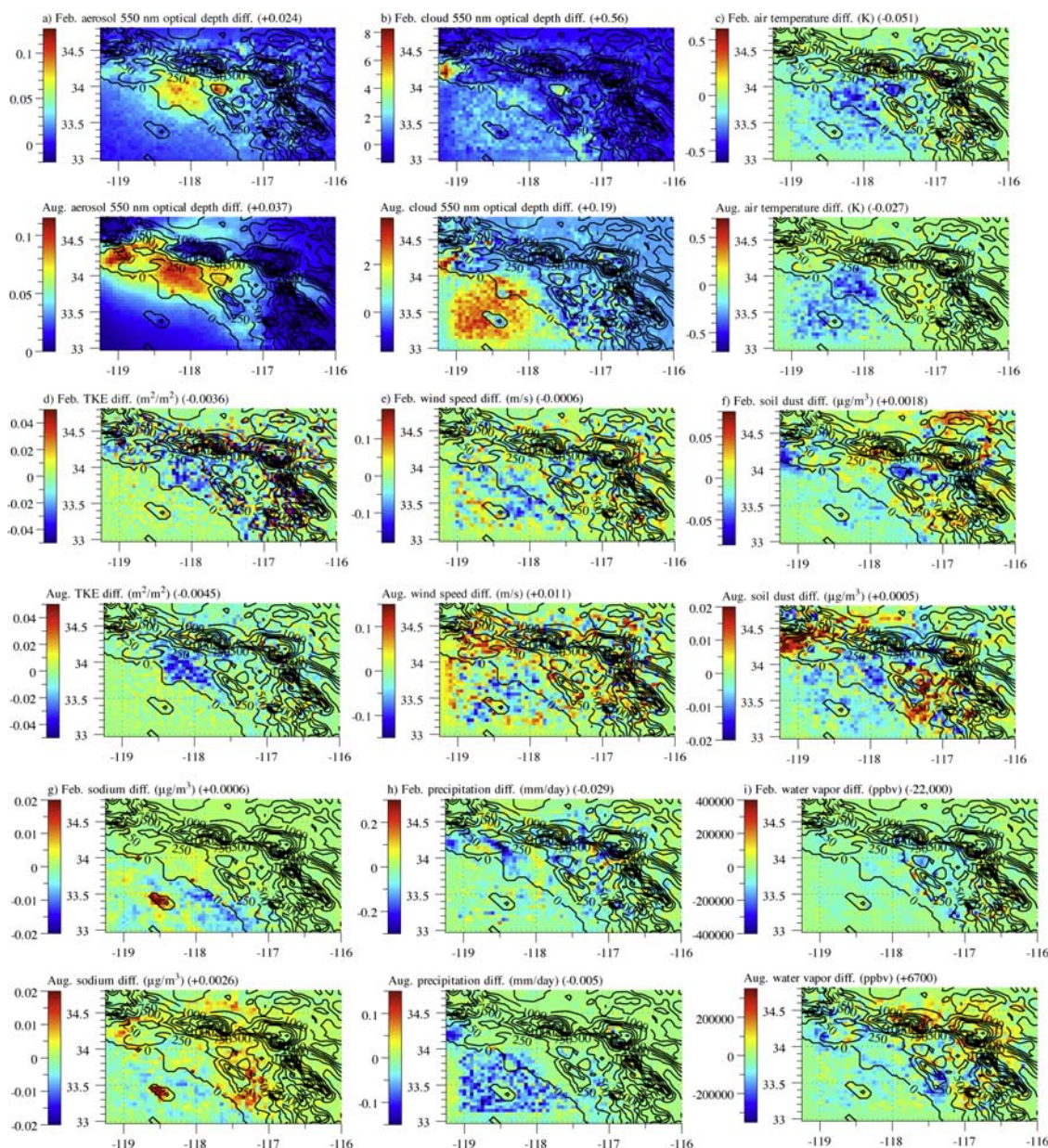


**Figure 1.** Modeled spatial difference between the baseline case (with AAPPG emissions) and the sensitivity case (no AAPPG emissions) in several parameters in the South Coast Air Basin domain, averaged over all hours of February and August 1999 when anthropogenic aerosol particles and their precursor gases (AAPPG) were present versus absent. The contours indicate topography in meters. Figures 1a, 1b, 1c, and 1h originate from Jacobson et al. (submitted manuscript, 2006) but are repeated here for convenience. All figures, except optical depth and precipitation, which are column-integrated, show near-surface values. Numbers in parentheses are average parameter values over all land points.

with hourly paired-in-time-and-space data for the SCAB domain.

### 3. Effects on Wind Speed and Wind Power

[7] Figure 1 here shows relevant model results. In both February and August, AAPPG increased aerosol optical depth (Figure 1a) and cloud optical depth (Figure 1b), decreasing near-surface air temperatures (Figure 1c), increasing stability, reducing turbulent kinetic energy (TKE) (Figure 1d), reducing the vertical transport of horizontal properties. Reduced TKE helped to reduce wind

speed over land near the coast (Figure 1e), increasing convergence of offshore winds flowing toward the coast, decreasing offshore wind speeds as well. Locations of wind speed decreases correlate with locations of aerosol-enhanced cloud optical depth increases (Figure 1b). Peak wind speed reductions were  $\sim 0.2$  m/s ( $\sim 7\%$  of the baseline) in both months. AAPPG increased some wind speeds in the mountains, away from increases in aerosol particles and clouds, particularly in August. These increases were due to pressure gradient changes from local temperature decreases due to AAPPG.

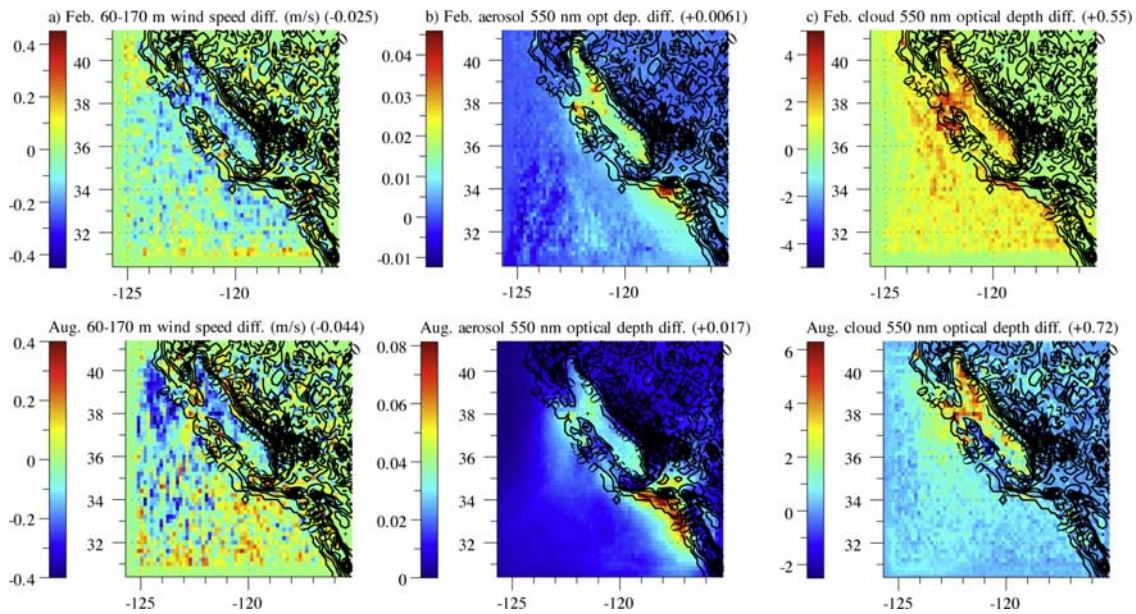


Figure 2. Same as Figure 1, but for parameters in the California domain.

[8] Reduced wind speeds due to AAPPG decreased emissions of wind-driven soil dust (Figure 1f) and sea spray particles (Figure 1g) in locations where wind speeds decreased. Whereas sea spray is relatively reflective, soil dust is reflective and absorbing. Since soil dust and sea spray decreases were triggered by AAPPG, decreases in soil dust and sea spray offset some enhanced reflection and absorption due to AAPPG.

[9] AAPPG reduced precipitation (Figure 1h) by (a) reducing wind speeds, which reduced water vapor advection from the ocean, (b) cooling surface air temperatures (Figure 1c), which reduced evaporation from soil and ocean water (Figure 1i), (c) spreading water over more aerosol particles, which slowed rain formation by collision/coalescence, allowing clouds to last longer and diffuse more, increasing cloud fraction here by about 3% in February and 0.3% in August (as in work by, e.g., Warner [1968], Albrecht [1989], Rosenfeld [2000], Borys et al.

[2003], Ackerman et al. [2003], Givati and Rosenfeld [2004], Andreae et al. [2004], and Koren et al. [2004, 2005]).

[10] To determine the robustness of the results, nested simulations were performed for California as a whole. Auxiliary Figure S1 compares base-model predictions with paired-in-time-and-space hourly data. Figure 2a here shows modeled changes in wind speed resulting from AAPPG 60–170 m above ground (encompassing hub heights of large wind turbines). The figure shows strong wind speed reductions in the Central Valley due to AAPPG. Reductions occurred primarily under enhanced aerosol optical depth (Figure 2b), but mostly in the northern Central Valley, where AAPPG increased cloud optical depths significantly (Figure 2c). Wind reductions were up to 0.4 m/s (4–8% of baseline wind speeds) in much of the Central Valley and many coastal locations.

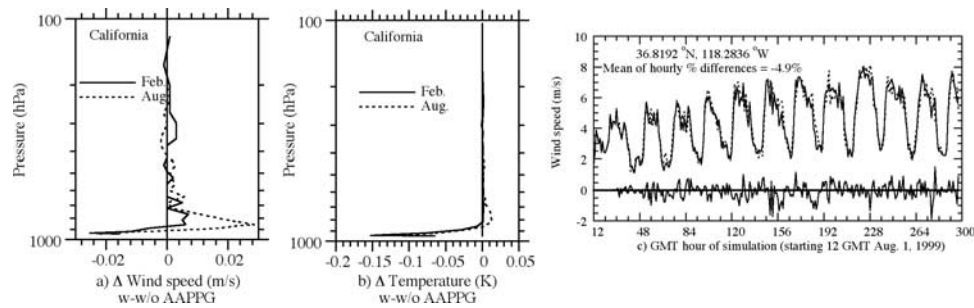


Figure 3. Differences (with minus without AAPPG emissions) in the modeled vertical profile of the California domain-averaged (a) wind speed and (b) temperature in February (solid line) and August (dashed line) 1999. (c) Modeled hourly wind speed with AAPPG emissions (solid line) and without such emissions (dashed line) and the difference between the two cases (isolated solid line) for 12 days in August at a specific location in California. A zero-change line is shown to compare the difference with. The “mean of hourly % differences” is  $100\% \times \sum_{i=1}^N (W_i - O_i) / NW_i$ , where  $W_i$  is the hourly value with AAPPG,  $O_i$  is the hourly value without AAPPG, and  $N$  is the number of hourly values.

[11] Although wind speed increases occurred in some places, they decreased on average in California between the surface and 900 hPa and increased above 900 hPa (Figure 3a), as expected since increased stability due to AAPPG (Figure 3b) reduced TKE, thus the vertical transport of horizontal momentum. Reduced wind speed also

reduced near-surface shear stress by up to  $0.03 \text{ kg/m}^2$  in the Central Valley during August, decreasing TKE and wind speeds further. Figure 3c shows that the average hourly change in wind speed over 12 days due to AAPPG (at 10 m) was  $-4.9\%$  at one location. Decreases occurred primarily during the day, consistent with expectations [e.g., *Zdunkowski and McQuage, 1972*]. Auxiliary Figure S4 shows results for other locations.

[12] Measurements between 1974 and 1994 from 79 stations in Southeast China show a 60 percent decrease in wind power (24 percent decrease in wind speed) [*Elliott et al., 2004*]. This “disappearing wind syndrome” was attributed mostly to new construction and vegetation growth around the meteorological stations. Applying the MODIS/NCEP analysis over Southeast China ( $116\text{--}118^\circ\text{E}$ ,  $24\text{--}34^\circ\text{N}$ ), we find that near-surface wind speeds decreased by  $0.8\%$  in February and  $10.2\%$  in August (average of  $-5.5\%$ ) when MODIS AODs increased from their lowest third to their highest third, suggesting again that a portion of decreasing winds correlates with increasing aerosol presence.

[13] China and California are increasing their wind energy use. The yearly-averaged energy production of most any wind turbine can be calculated within a few percent of manufacturer power curve data with  $E(\text{kWh/yr}) = P \times 8760 \times (0.087V - P/D^2)$  [*Masters, 2004; Jacobson and Masters, 2001*], where  $P$  is rated power (kW),  $V$  is the annual average Rayleigh-distributed wind speed (m/s) at hub height,  $D$  is rotor diameter (m), and 8760 is hrs/yr. The equation is empirical, so units do not equate. A conservative estimate of the wind speed reduction due to AAPPG from this study is  $1\text{--}5\%$ , with an upper limit of  $8\%$ . Wind turbines are placed optimally where the mean annual wind speed at hub height is  $>6.9 \text{ m/s}$  [*Jacobson and Masters, 2001*]. Applying a  $1\text{--}5\%$  reduction in wind speed to a baseline  $7 \text{ m/s}$  speed gives  $6.93\text{--}6.65 \text{ m/s}$ , resulting in annual wind energy losses of  $1.7\text{--}8.6\%$ , affecting wind energy’s competitiveness and ability to address climate change and air pollution.

#### 4. Effects on Precipitation and Water Supply

[14] Figure 4a compares modeled with measured [Lopez and Franco, 2006] baseline (w/AAPPG) California precipitation in February, 1999. Observed high precipitation along the northern coast and Sierra-Nevada range and low precipitation in Southern California were emulated by the model. The greatest modeled decreases in February precipitation due to AAPPG were in the northern

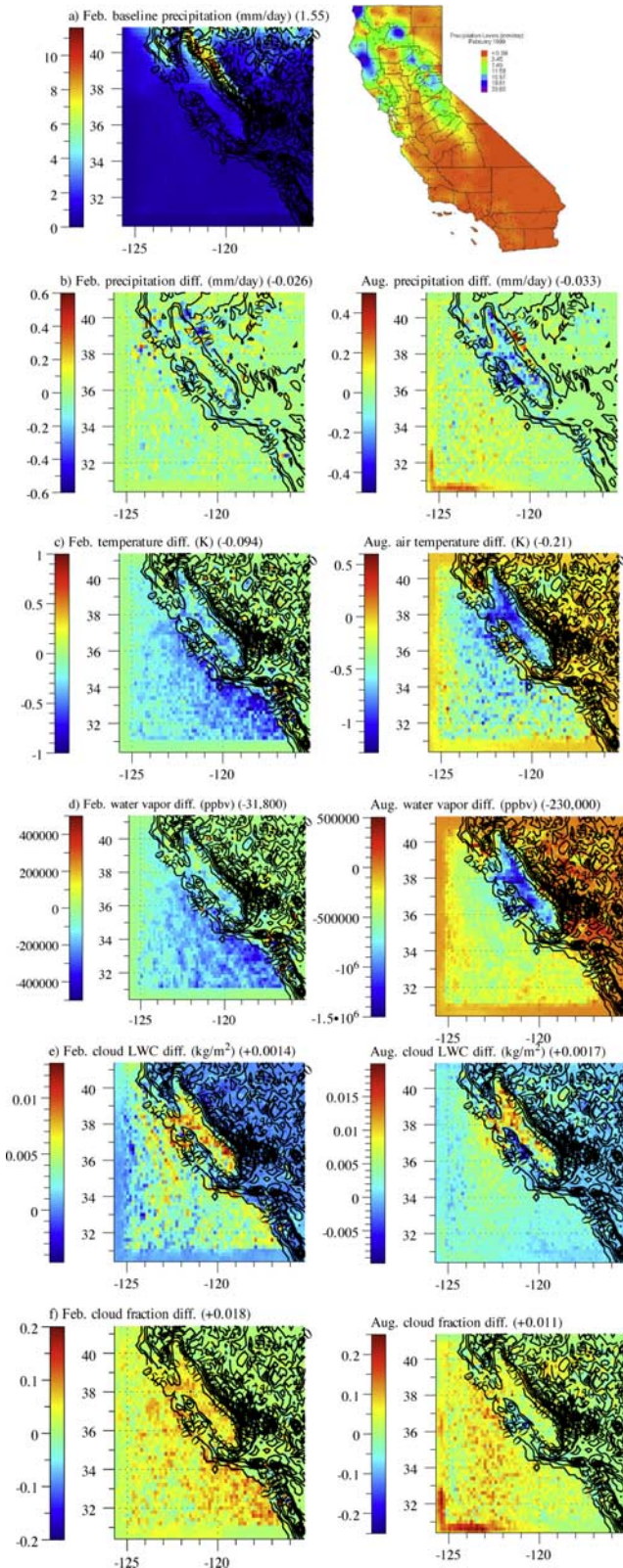


**Figure 4.** (a) Modeled and measured [Lopez and Franco, 2006] baseline (w/AAPPG) California precipitation in February, 1999. (b–f) Modeled spatial difference in California precipitation and additional parameters (continuing from Figure 2) in February and August 1999 when AAPPG emissions were present versus absent. The contours indicate topography. Contours for the difference plots are sparser than those of the baseline case to improve visualization in the mountains. Temperature and water vapor maps are near-surface maps. Numbers in parentheses are average parameter values over all land points.

Sierra Nevada Mountains (Figure 4b), where most precipitation occurred (Figure 4a). Modeled decreases were mostly on the upslope sides of mountains, a result consistent with a previous correlation study [Givati and Rosenfeld, 2004]. Decreases in August precipitation (drizzle and fog deposits) due to AAPPG were primarily in the Central Valley (Figure 4b).

[15] As in SCAB, AAPPG reduced California precipitation by reducing wind speeds (Figure 2a) and temperatures (Figure 4c), reducing near-surface water vapor (Figure 4d). Because AAPPG decreased cloud radius, clouds lasted longer, increasing cloud liquid water (Figure 4e), cloud fraction (Figure 4e) and cloud optical depth (Figure 2c). Satellite analysis supports the modeled positive correlations between AOD and both cloud liquid and cloud fraction [Koren *et al.*, 2005].

[16] Precipitation reduction due to AAPPG affects water supply. California receives 193 million acre-feet (MAF) of precipitation annually (1.54 mm/day). Agriculture, households, and industry use about 24.9 MAF of this (12.9%) (Association of California Water Agencies, 2005, <http://www.acwanet.com>) (hereinafter referred to as ACWA website). The modeled AAPPG-induced precipitation decrease over land in California during February 1999 was 0.03 mm/day, or 2% of the baseline 1.5 mm/day precipitation over land. However, the reduction over much of the Sierras, where most precipitation falls, was up to 0.5 mm/day, or 4–5% of the baseline 10–13 mm/day there.

[17] Although AAPPG also reduced evaporation, only part of this reduction affects water supply. Once water reaches a reservoir, which is deep, only the surface water evaporates. Since the surface area among all reservoirs is small relative to California, increases in reservoir water due to reduced evaporation offset little precipitation loss, which occurs over a large area.

[18] Although a one-year precipitation loss has little effect on water supply, an annual 2–5% precipitation loss may decrease water to reservoirs by 0.5–1.25 MAF/yr. California's population may reach 40 million by 2010, requiring an additional 4–6 MAF by then (ACWA website). Since aerosol particles contribute to the strain in water supply in California, reducing particle emissions will ameliorate this problem.

## 5. Summary

[19] Aerosol particles and aerosol-enhanced clouds reduce wind speeds below them by stabilizing the air, reducing the vertical transport of horizontal momentum. This conclusion was reached in two ways: through a correlation study using MODIS satellite and NCEP reanalysis information and through numerical model experiments. Reduced wind speeds, reduced evaporation, and increased cloud lifetime due to AAPPG reduced precipitation in Los Angeles and California as a whole. The result was not sensitive to the turbulence parameterization used, as illustrated by a sensitivity test in the auxiliary material. Reduced wind speeds also reduce wind-turbine electricity potential; reduced precipitation reduces water supply and hydroelectric power. Thus, aerosol pollution acts in a positive feedback to reduce clean

energy available to reduce emissions of aerosol particles and their precursor gases.

[20] **Acknowledgments.** This paper is dedicated to the memory of Yoram Kaufman, who passed away during our writing of it. This work was supported by California Energy Commission's (CEC's) Public Interest Energy Research (PIER) program and by NASA under grants NNG04GE93G and NNG04GJ89G. We would like to thank Guido Franco and Gina Lopez of the CEC and Shana Mattoo of NASA GSFC for comments and technical assistance.

## References

- Ackerman, A. S., O. B. Toon, D. E. Stevens, and J. A. Coakley Jr. (2003), Enhancement of cloud cover and suppression of nocturnal drizzle in stratocumulus polluted by haze, *Geophys. Res. Lett.*, *30*(7), 1381, doi:10.1029/2002GL016634.
- Ackerman, T. P. (1977), A model of the effect of aerosols on urban climates with particular applications to the Los Angeles basin, *J. Atmos. Sci.*, *34*, 531–546.
- Ackerman, T. P., K.-N. Liou, and C. B. Leovy (1976), Infrared radiative transfer in polluted atmospheres, *J. Appl. Meteorol.*, *15*, 28–35.
- Albrecht, B. A. (1989), Aerosols, cloud microphysics, and fractional cloudiness, *Science*, *245*, 1227–1230.
- Andreae, M. O., D. Rosenfeld, P. Artaxo, A. A. Costa, G. P. Frank, K. M. Longo, and M. Z. F. Silva-Dias (2004), Smoking rain clouds over the Amazon, *Science*, *303*, 133–134.
- Archer, C. L., and M. Z. Jacobson (2003), Spatial and temporal distributions of U.S. winds and wind power at 80 m derived from measurements, *J. Geophys. Res.*, *108*(D9), 4289, doi:10.1029/2002JD002076.
- Arya, S. P. (1988), *Introduction to Micrometeorology*, 307 pp., Elsevier, New York.
- Bergstrom, R. W., and R. Viskanta (1973), Modeling of the effects of gaseous and particulate pollutants in the urban atmosphere: Part I. Thermal structure, *J. Appl. Meteorol.*, *12*, 901–912.
- Borys, R. D., D. H. Lowenthal, S. A. Cohn, and W. O. J. Brown (2003), Mountaintop and radar measurements of anthropogenic aerosol effects on snow growth and snowfall rate, *Geophys. Res. Lett.*, *30*(10), 1538, doi:10.1029/2002GL016855.
- Elliott, D., M. Schwartz, and G. Scott (2004), Wind resource base, in *Encyclopedia of Energy*, vol. 6, pp. 465–479, Elsevier, New York.
- Givati, A., and D. Rosenfeld (2004), Quantifying precipitation suppression due to air pollution, *J. Appl. Meteorol.*, *43*, 1038–1056.
- Jacobson, M. Z. (1997), Development and application of a new air pollution modeling system. Part III: Aerosol-phase simulations, *Atmos. Environ., Part A*, *31*, 587–608.
- Jacobson, M. Z. (1998), Studying the effects of aerosols on vertical photolysis rate coefficient and temperature profiles over an urban airshed, *J. Geophys. Res.*, *103*, 10,593–10,604.
- Jacobson, M. Z. (2001), GATOR-GCMM: A global through urban scale air pollution and weather forecast model: 1. Model design and treatment of subgrid soil, vegetation, roads, rooftops, water, sea ice, and snow, *J. Geophys. Res.*, *106*, 5385–5402.
- Jacobson, M. Z. (2002), Control of fossil-fuel particulate black carbon plus organic matter, possibly the most effective method of slowing global warming, *J. Geophys. Res.*, *107*(D19), 4410, doi:10.1029/2001JD001376.
- Jacobson, M. Z. (2003), Development of mixed-phase clouds from multiple aerosol size distributions and the effect of the clouds on aerosol removal, *J. Geophys. Res.*, *108*(D8), 4245, doi:10.1029/2002JD002691.
- Jacobson, M. Z. (2004), The climate response of fossil-fuel and biofuel soot, accounting for soot's feedback to snow and sea ice albedo and emissivity, *J. Geophys. Res.*, *109*, D21201, doi:10.1029/2004JD004945.
- Jacobson, M. Z., and G. M. Masters (2001), Exploiting wind versus coal, *Science*, *293*, 1438.
- Koren, I., Y. J. Kaufman, L. A. Remer, and J. V. Martins (2004), Measurements of the effect of Amazon smoke on inhibition of cloud formation, *Science*, *303*, 342–345.
- Koren, I., Y. J. Kaufman, D. Rosenfeld, L. A. Remer, and Y. Rudich (2005), Aerosol invigoration and restructuring of Atlantic convective clouds, *Geophys. Res. Lett.*, *32*, L14828, doi:10.1029/2005GL023187.
- Lopez, G., and G. Franco (2006), Precipitation maps of California from Western Regional Climate Center Data, maps, Calif. Energy Comm., Sacramento.
- Masters, G. M. (2004), *Renewable and Efficient Electric Power Systems*, 654 pp., John Wiley, Hoboken, N. J.

- Riehl, H. (1972), *Introduction to the Atmosphere*, 516 pp., McGraw-Hill, New York.
- Rosenfeld, D. (2000), Suppression of rain and snow by urban and industrial air pollution, *Science*, 287, 1793–1796.
- Venkatram, A., and R. Viskanta (1977), Effects of aerosol-induced heating on the convective boundary layer, *J. Atmos. Sci.*, 34, 1918–1933.
- Warner, J. (1968), A reduction in rainfall associated with smoke from sugar-cane fires—An inadvertent weather modification?, *J. Appl. Meteorol.*, 7, 247–251.
- Zdunkowski, W. G., and N. D. McQuage (1972), Short-term effects of aerosols on the layer near the ground in a cloudless atmosphere, *Tellus*, 24, 237–254.
- Zdunkowski, W. G., R. M. Welch, and J. Paegle (1976), One dimensional numerical simulation of the effects of air pollution on the planetary boundary layer, *J. Atmos. Sci.*, 33, 2399–2414.

---

M. Z. Jacobson, Department of Civil and Environmental Engineering, Stanford University, Stanford, CA 94305-4020, USA. (jacobson@stanford.edu)